Electron-capture rates in medium-mass nuclei within deformed quasiparticle random-phase approximation(QRPA)

Eun Ja Ha

Department of physics, Hanyang University, Seoul, Korea

in collaboration with

Myung-Ki Cheoun[1] , Hiroyuki Sagawa[2], and Gianluca Colò[3]

1) Origin of Matter and Evolution of Galaxy (OMEG) Institute & Soongsil University, Seoul, Korea
2) RIKEN and University of Aizu, Japan
3) Dipartimento di Fisica, Universit`a degli Studi and INFN, Milano, Italy

❖ Contents

1. Introduction & Formalism

- Electron capture(EC) rate & Gamow-Teller(GT) transition

2. Result : Impact of nuclear deformation on stellar weak rates

- Electron capture rates of ^{48}Ti, ^{56}Ni, ^{60}Ge, and ^{64}Zn

3. Summary

❖ Rapid proton-capture(rp) process

AI-generated

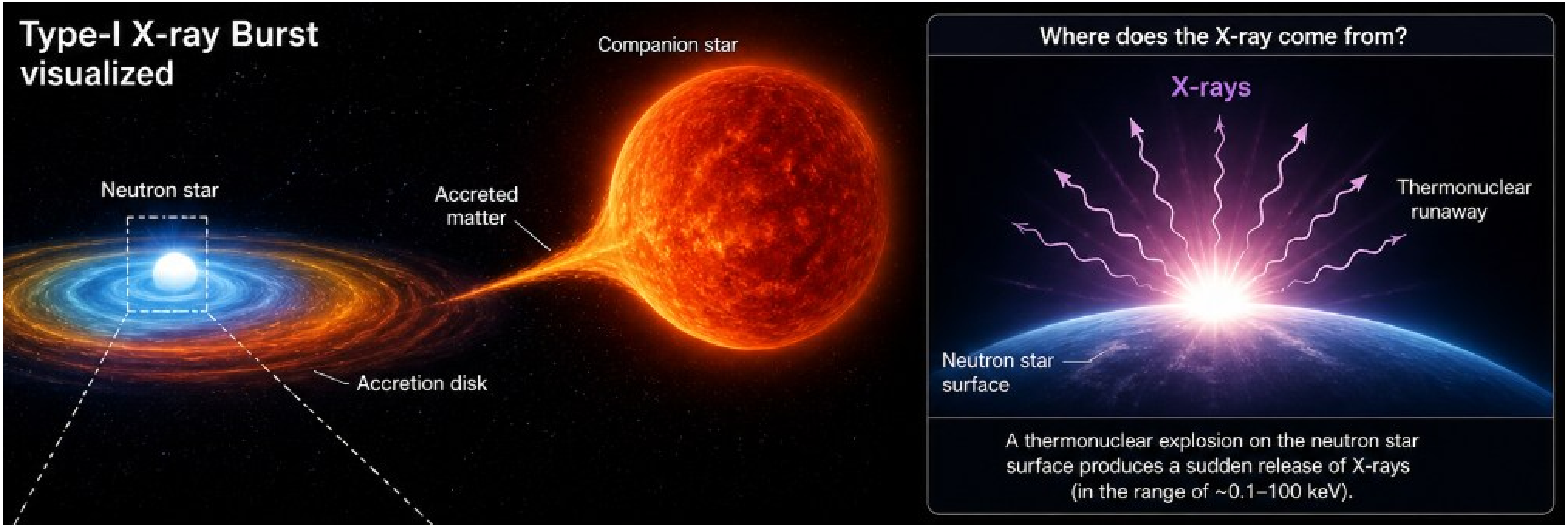

- Type-I X-ray bursts are thermonuclear explosions that occur on neutron stars accreting matter.
- These bursts are powered by the rapid proton-capture (rp) process, which proceeds through repeated proton captures and weak decays.
- The rp-process proceeds through proton-rich nuclei near the N = Z line.

❖ Proton-rich(neutron deficient) nuclei

- The rp-process flow is significantly slowed down at the waiting-point nuclei such as ^{64}Ge.

β⁺ decay half-life: 63.7 s

Nature Physics 19, 1234–1238 (2023)

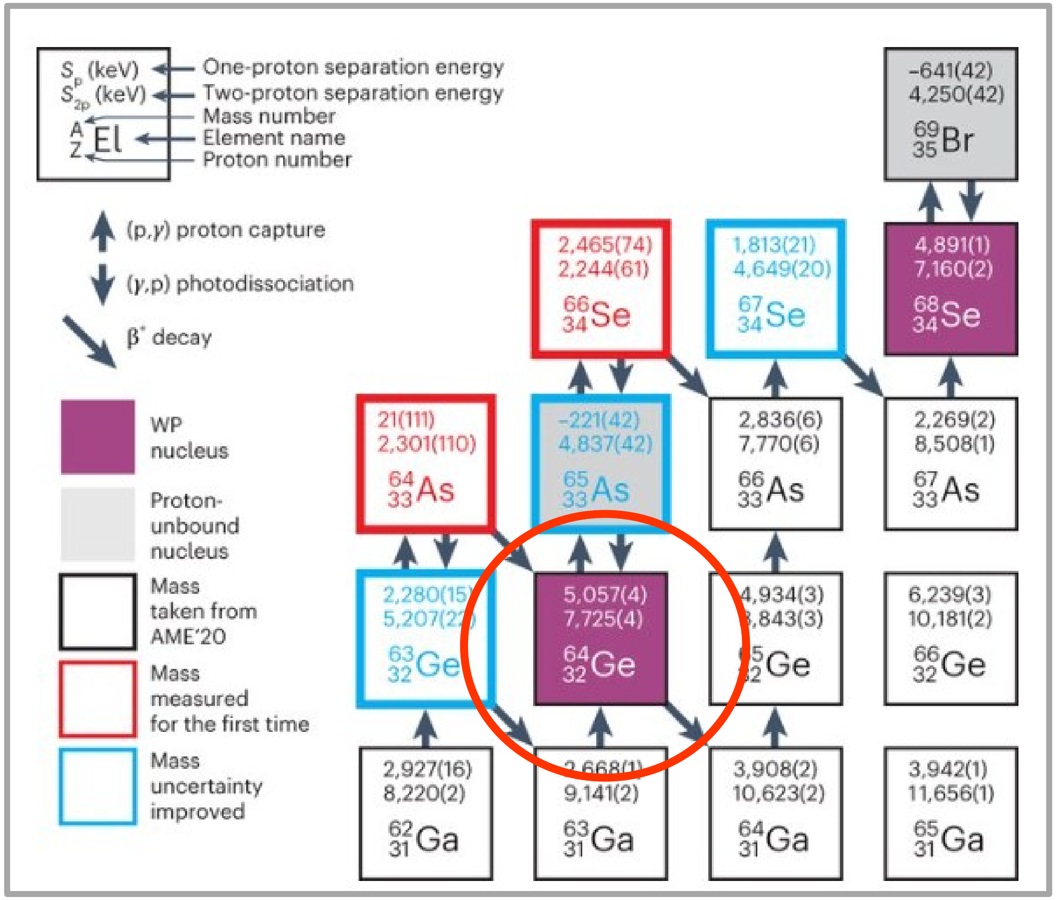

- Proton capture is hindered, creating a bottleneck that must be bypassed by the relatively slow β⁺ decay.
- Proton–rich nuclei become stable by converting a proton into a neutron.

Z → Z-1

β⁺ decay : Q-value, nuclear matrix element

$$p \rightarrow n + e^+ + \nu_e$$

$$(Z, A)_i \rightarrow (Z-1, A)_f + e^+ + \nu_e$$

Electron capture : ρY_e, T, μ_e

$$p + e^- \rightarrow n + \nu_e$$

$$e^- + (Z, A)_i \rightarrow (Z-1, A)_f + \nu_e$$

✓ At sufficiently high temperature and density, continuum electron capture significantly contributes to the total weak-reaction rate and can compete with β⁺ decay.

❖ Why is electron capture(EC) important?

- Electrons(green dots) are captured by the nuclei(**neon fish**)

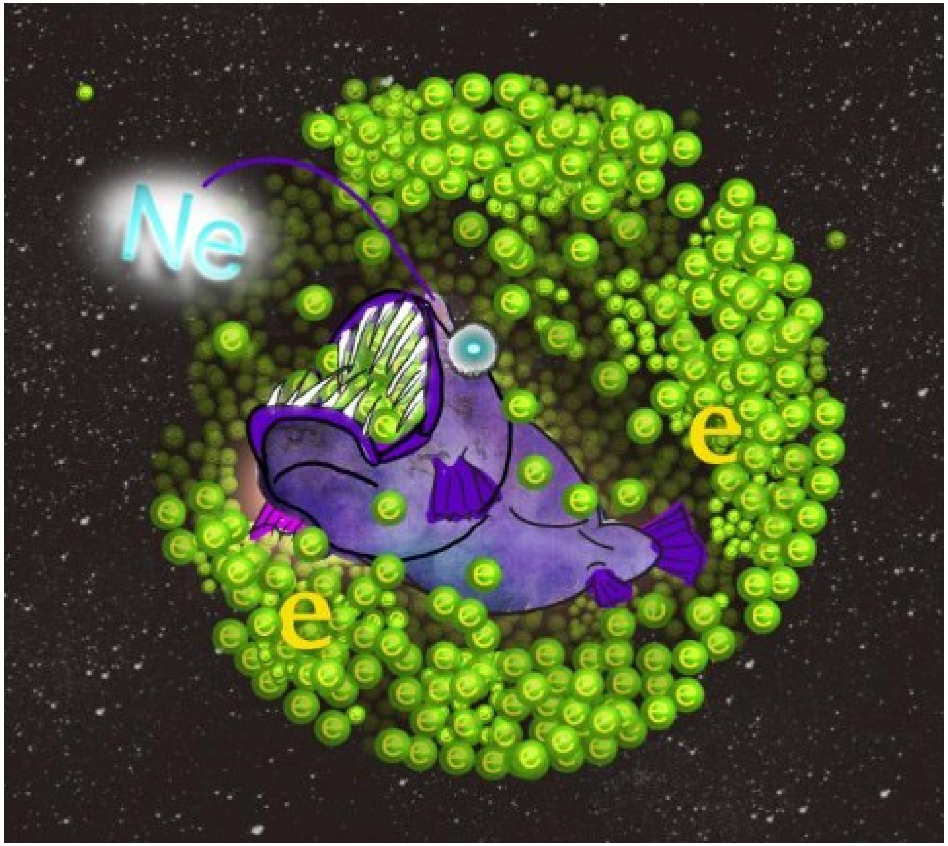

@IPMU

- Electron capture(EC)

  $p + e^- \rightarrow n + \nu_e$

  $e^- + (Z, A)_i \rightarrow (Z-1, A)_f + \nu_e$

- Decreases **electron fraction** $Y_e = \frac{\#\ \text{of electron}}{\#\ \text{of baryon}}$

  →reduces electron degeneracy pressure

- Weakens pressure support against gravity

- Triggers **core collapse**

- Leads to: supernova explosion & formation of a neutron star

✓ Reliable EC rates on medium-mass and heavy nuclei are indispensable ingredients in astrophysical simulations of stellar evolution and supernova dynamics.

❖ Stellar electron-capture rate $e^- + (Z, A)_i \rightarrow (Z-1, A)_f + \nu_e$

Neutrinos are assumed to escape freely, neutrino blocking(neutrino occupation) is neglected.

In a stellar environment, the total EC rate is obtained as a thermal average over the populated parent states,

$$\lambda = \sum_i P_i \lambda_i, \qquad P_i = \frac{(2J_i + 1)\exp(-E_i/kT)}{G}, \qquad G = \sum_i (2J_i + 1)\exp(-E_i/kT), \tag{12}$$

thermal population factor

where J_i and E_i are the spin and excitation energy of the parent state, and G is the nuclear partition function. The rate from a given parent state is

$$\lambda_i = \sum_f \lambda_{if}. \tag{13}$$

In the present calculations, however, we restrict ourselves to transitions built on the parent ground state and therefore use $P_0 = 1$, but $0 \leq P_{(i \neq 1)} \leq 1$ in finite temperature. Within the allowed approximation, the partial EC rate from an initial state i to a final state f can be written in the standard form,

$$\lambda_{if} = \frac{\ln 2}{D} B_{if}\, \Phi_{if}(\rho, T), \qquad D = 6146 \text{ s}, \tag{14}$$

where B_{if} is the reduced transition strength and Φ_{if} is the phase-space factor. In general,

$$B_{if} = B(F)_{if} + B(\mathrm{GT})_{if}, \tag{15}$$

with

$$B(F)_{if} = \frac{1}{2J_i + 1} \left| \left\langle f \left\| \sum_k \tau_k^{\pm} \right\| i \right\rangle \right|^2, B(\mathrm{GT})_{if} = \frac{1}{2J_i + 1} \left| \left\langle f \left\| \sum_k \sigma_k \tau_k^{\pm} \right\| i \right\rangle \right|^2. \tag{16}$$

The Fermi contribution is expected to be small, and the EC rates in this work are dominated by allowed GT^+ transitions.

Using the standard dimensionless variables

$$\omega = \frac{E_e}{m_e c^2}, \qquad p = \sqrt{\omega^2 - 1}, \qquad \theta = \frac{kT}{m_e c^2}, \tag{17}$$

the phase-space factor can be written as

$$\Phi_{if}(\rho, T) = \int_{\omega_l}^{\infty} \omega p \,(Q_{if} + \omega)^2 F(Z, \omega) S_e(\omega)\, d\omega, \tag{18}$$

where $F(Z, \omega)$ is the Fermi function accounting for the Coulomb distortion of the electron wave function, and $S_e(\omega)$ is the electron occupation probability. The transition energy entering the neutrino phase space is defined as

$$Q_{if} = \frac{Q_{\mathrm{EC}} - m_e c^2 + E_i - E_f}{m_e c^2}, \tag{19}$$

effective neutrino energy in electron capture

For the Coulomb correction we use the usual Fermi-function approximation

$$F(Z, \omega) = \frac{2\pi\eta}{1 - \exp(-2\pi\eta)}, \qquad \eta = \alpha Z \frac{\omega}{p}, \tag{21}$$

where α is the fine-structure constant. The electron occupation probability is given by the Fermi–Dirac distribution

$$S_e(\omega) = \frac{1}{\exp[(\omega - \mu_e)/\theta] + 1}, \tag{22}$$

where μ_e is the electron chemical potential in units of $m_e c^2$. The corresponding positron occupation probability is

$$S_{e^+}(\omega) = \frac{1}{\exp[(\omega + \mu_e)/\theta] + 1}. \tag{23}$$

The electron chemical potential is determined self-consistently from the stellar density through

$$\rho Y_e = \frac{1}{\pi^2 N_A} \left(\frac{m_e c}{\hbar}\right)^3 \int_0^{\infty} [S_e(\omega) - S_{e^+}(\omega)]\, p^2 dp, \tag{24}$$

❖ Gamow-Teller(GT) transition

Gamow-Teller transition and Charge-Exchange (CE) reactions at 100-300 MeV

$\Delta T=1$, $\Delta S=1$, $\Delta L=0$ induced by $\vec{\sigma}\, t_{\pm}$

strength : **B(GT)**

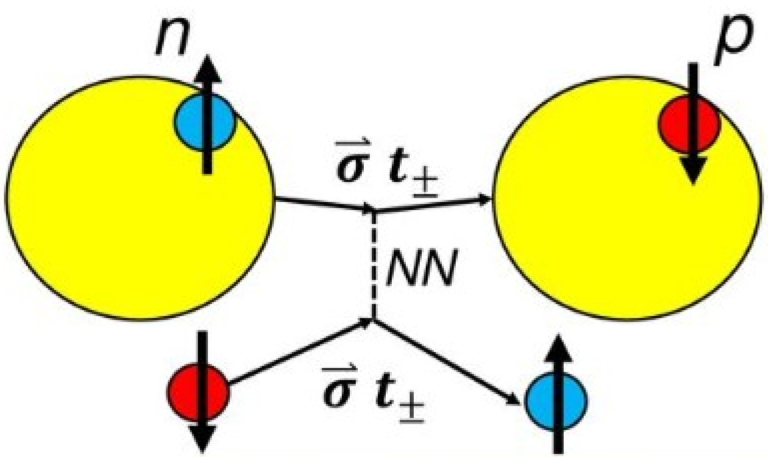

(p,n), (^{3}He,t), (n,p), (t,^{3}He), …

100 – 300 MeV
→ Isovector spin-flip >> Isovector nonspin-flip
& DWIA good

$$\left(\frac{d\sigma}{d\Omega}(q=0)\right)_{(p,n)} = \hat{\sigma}\, B(GT)$$

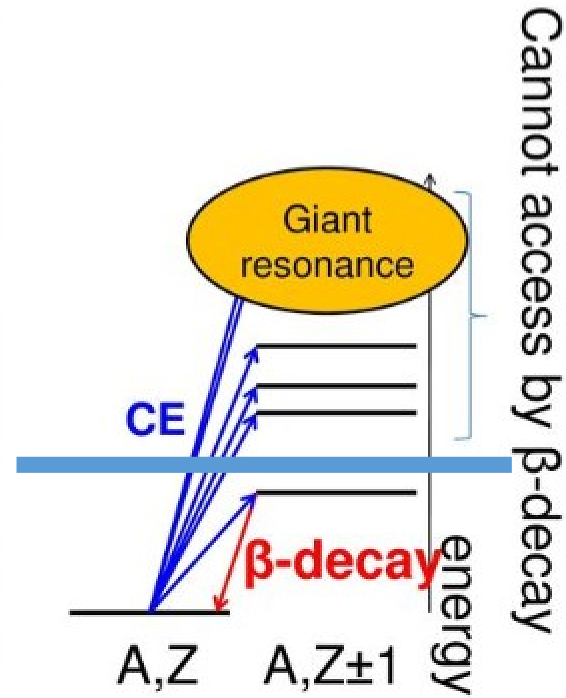

(p,n) reaction is an inverse kinematics.

Any (0-50 MeV) Ex!

From M. Sasano's talk

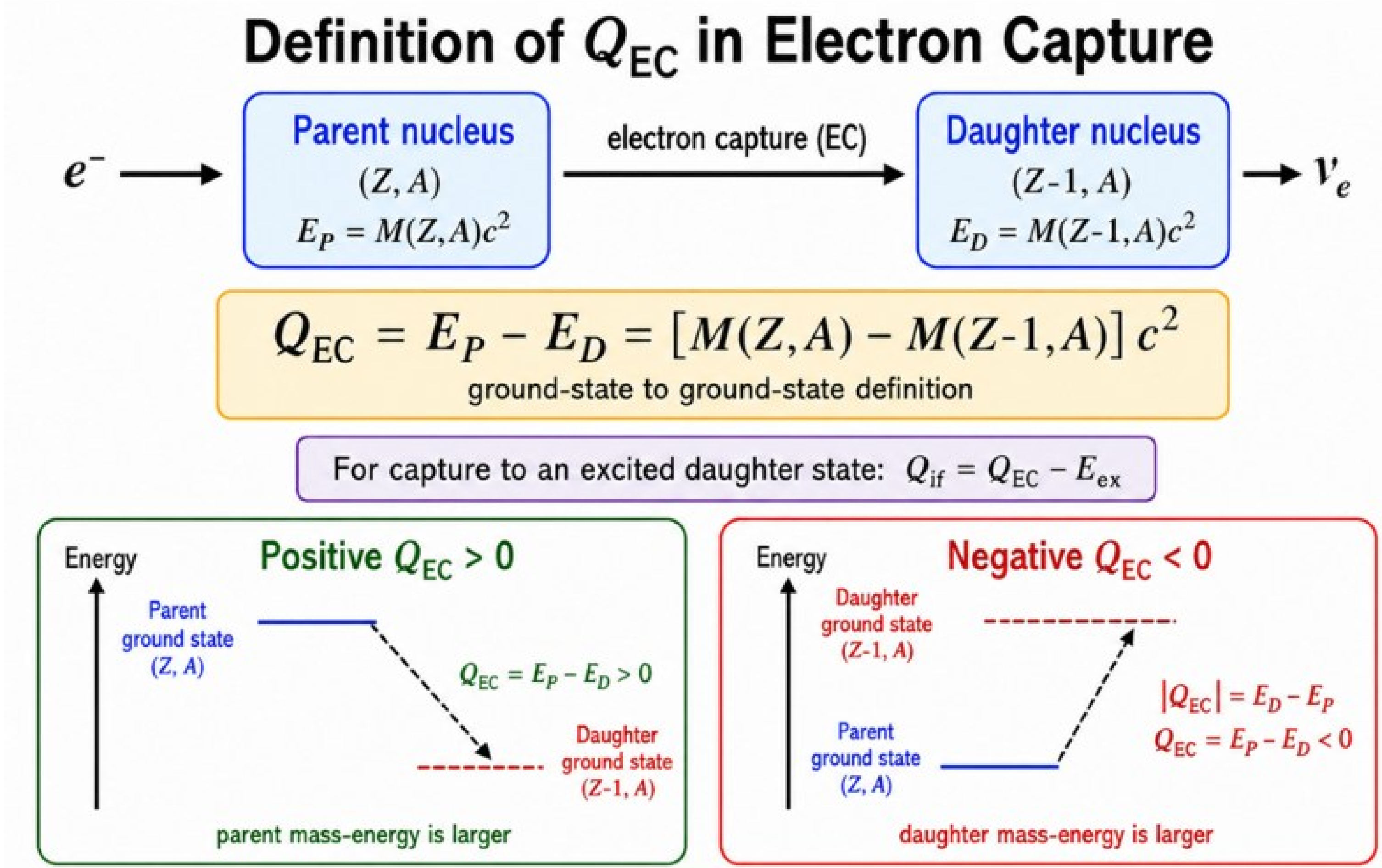

EC is always energetically allowed **EC requires high-energy electrons**

TABLE II: Ground-state-to-ground-state electron-capture $Q_{\rm EC}$ values (MeV) used in the phase-space integrals, obtained from experimental nuclear masses [36].

Nucleus	^{48}Ti	^{56}Ni	^{60}Zn	^{64}Ge
Q_{EC}[MeV]	-3.990	2.132	4.170	4.517

❖ Formalism

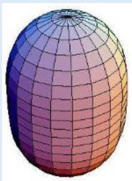

SHFB (T=1)
nn+pp

→

pn-DQRPA

G-matrix for residual interactions
(Bonn potential)

parameter free !!!

3 Skyrme Hartree-Fock-Bogoliubov Method

3.1 Skyrme Energy Density Functional

For Skyrme forces, the HFB energy (6) has the form of a local energy density functional,

$$E[\rho,\tilde{\rho}] = \int d^3\mathbf{r}\ \mathcal{H}(\mathbf{r}), \tag{9}$$

where

$$\mathcal{H}(\mathbf{r}) = H(\mathbf{r}) + \tilde{H}(\mathbf{r}) \tag{10}$$

is the sum of the mean-field and pairing energy densities. In the present implementation, we use the following explicit forms:

$$\begin{aligned} H(\mathbf{r}) \ = \ & \tfrac{\hbar^2}{2m}\tau + \tfrac{1}{2}t_0\left[\ \left(1+\tfrac{1}{2}x_0\right)\rho^2 - \left(\tfrac{1}{2}+\ x_0\right)\sum_q \rho_q^2\ \right] \\ + \ & \tfrac{1}{2}t_1\left[\ \left(1+\tfrac{1}{2}x_1\right)\rho\left(\tau - \tfrac{3}{4}\,\Delta\rho\right)\right] - \left(\tfrac{1}{2}+\ x_1\right)\sum_q \rho_q\left(\tau_q - \tfrac{3}{4}\Delta\rho_q\right)\Big] \\ + \ & \tfrac{1}{2}t_2\left[\ \left(1+\tfrac{1}{2}x_2\right)\rho\left(\tau + \tfrac{1}{4}\Delta\rho\right) - \left(\tfrac{1}{2}+\ x_2\right)\sum_q \rho_q\left(\tau_q + \tfrac{1}{4}\Delta\rho_q\right)\right] \\ + \ & \tfrac{1}{12}t_3\rho^\alpha\left[\left(1+\tfrac{1}{2}x_3\right)\rho^2 - \left(x_3+\tfrac{1}{2}\right)\sum_q \rho_q^2\right] \\ - \ & \tfrac{1}{8}\left(t_1x_1+t_2x_2\right)\sum_{ij}\mathbf{J}_{ij}^2 + \tfrac{1}{8}\left(t_1-t_2\right)\sum_{q,ij}\mathbf{J}_{q,ij}^2 \\ - \ & \tfrac{1}{2}W_0\sum_{ijk}\varepsilon_{ijk}\left[\rho\nabla_k\mathbf{J}_{ij} + \sum_q \rho_q\nabla_k\mathbf{J}_{q,ij}\right] \end{aligned} \tag{11}$$

and

$$\tilde{H}(\mathbf{r}) = \tfrac{1}{2}V_0\left[1 - V_1\left(\frac{\rho}{\rho_0}\right)^\gamma\ \right]\sum_q \tilde{\rho}_q^2. \tag{12}$$

Index q labels the neutron ($q=n$) or proton ($q=p$) densities, while densities without index q denote the sums of proton and neutron densities. $H(\mathbf{r})$ and $\tilde{H}(\mathbf{r})$ depend on the particle local density $\rho(\mathbf{r})$, pairing local density $\tilde{\rho}(\mathbf{r})$, kinetic energy density $\tau(\mathbf{r})$, and spin-current density $\mathbf{J}_{ij}(\mathbf{r})$:

❖ Numerical details

- HFBTHO(v1.66p)
- Number of oscillator shell : N_{sh}=18
- Pairing energy cut(pwi:pairing window) : E_{cut}=60MeV
- Mixed pairing(volume + surface pairing)
- Without Lipkin-Nogami(LN) correction
- SGII

From T. Naito

表 3.1: Pairing strength (MeV fm^3)

Interaction	w/o Lipkin-Nogami Correction		w/ Lipkin-Nogami Correction	
	Volume-type pairing	Mixed-type pairing	Volume-type pairing	Mixed-type pairing
SAMi	213.7	322.4	196.1	302.7
SLy4	194.2	295.3	184.3	283.8
SLy5	188.2	288.8	181.0	280.0
SkM*	156.2	246.2	152.7	242.1
SGII	169.8	266.5	163.2	258.0
SkP	136.5	220.2	133.2	215.7

❖ Potential energy curve (PEC) of ^{48}Ti, ^{56}Ni, ^{60}Zn, and ^{64}Ge

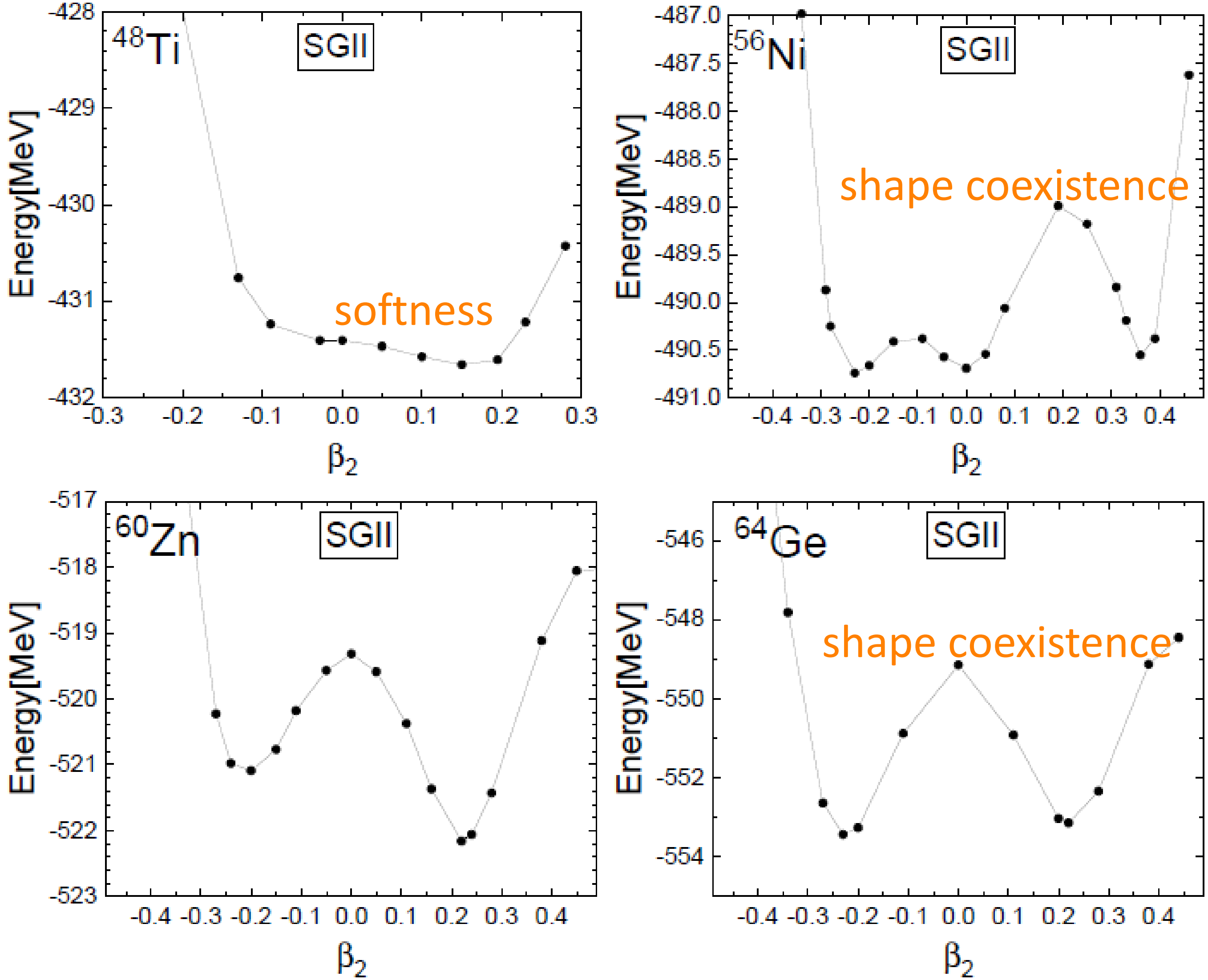

Softness : flat potential-energy surface where different nuclear deformations have similar energies.
Shape coexistence: different intrinsic shapes, such as spherical, prolate, or oblate configurations, coexist at similar energies in the same nucleus.

❖ GT strength B(GT) of ^{48}Ti

- Comparison of $\beta_2 = 0$ and 0.15 tests the shape dependence of spin-isospin properties.

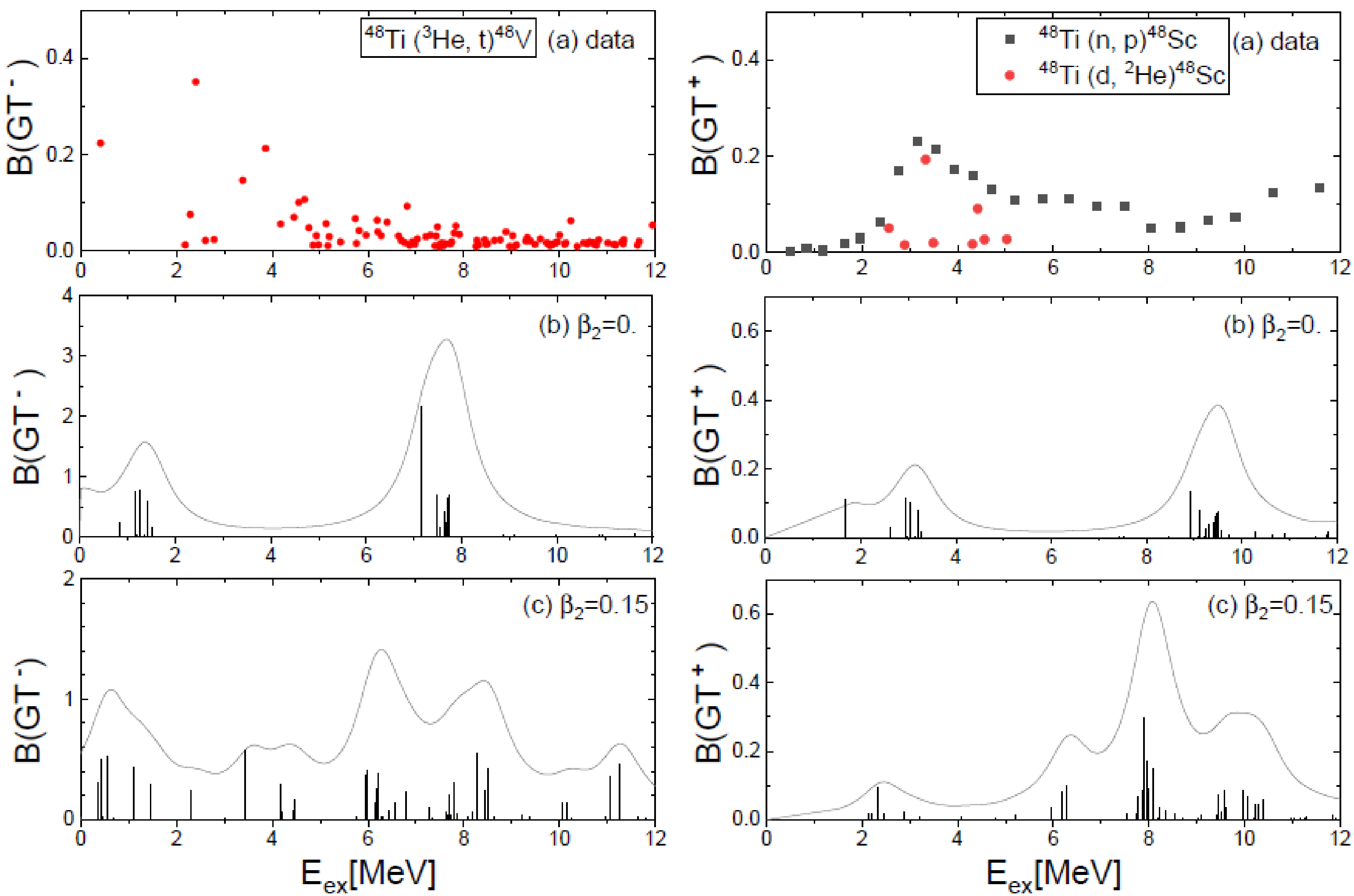

Quenching factor q=0.79,
[PRC 91, 024317 (2015)]

✓ The GT⁻ response of ^{48}Ti suggests that this nucleus is shape-soft (not fixed to a specific shape) rather than rigidly spherical or strongly deformed.

❖ Cumulative sum ΣB(GT) of ^{48}Ti

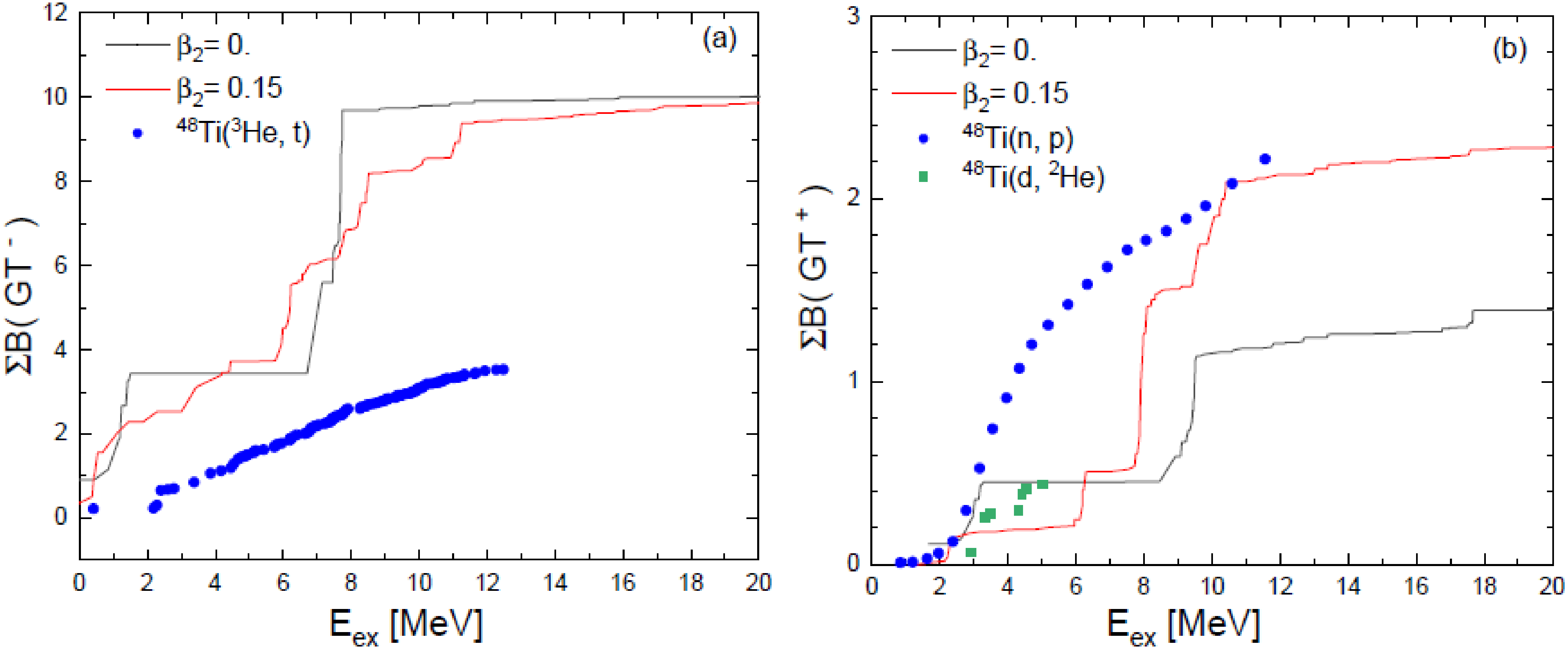

- ✓ Cumulated sum of GT$^-$ overestimate about twice the data and larger than the results by the shell model.
- ✓ GT$^\pm$ data also do not satisfy the Ikeda sum rule(ISR). More systematic analysis are necessary for the differences.

❖ EC rate of ^{48}Ti

preliminary

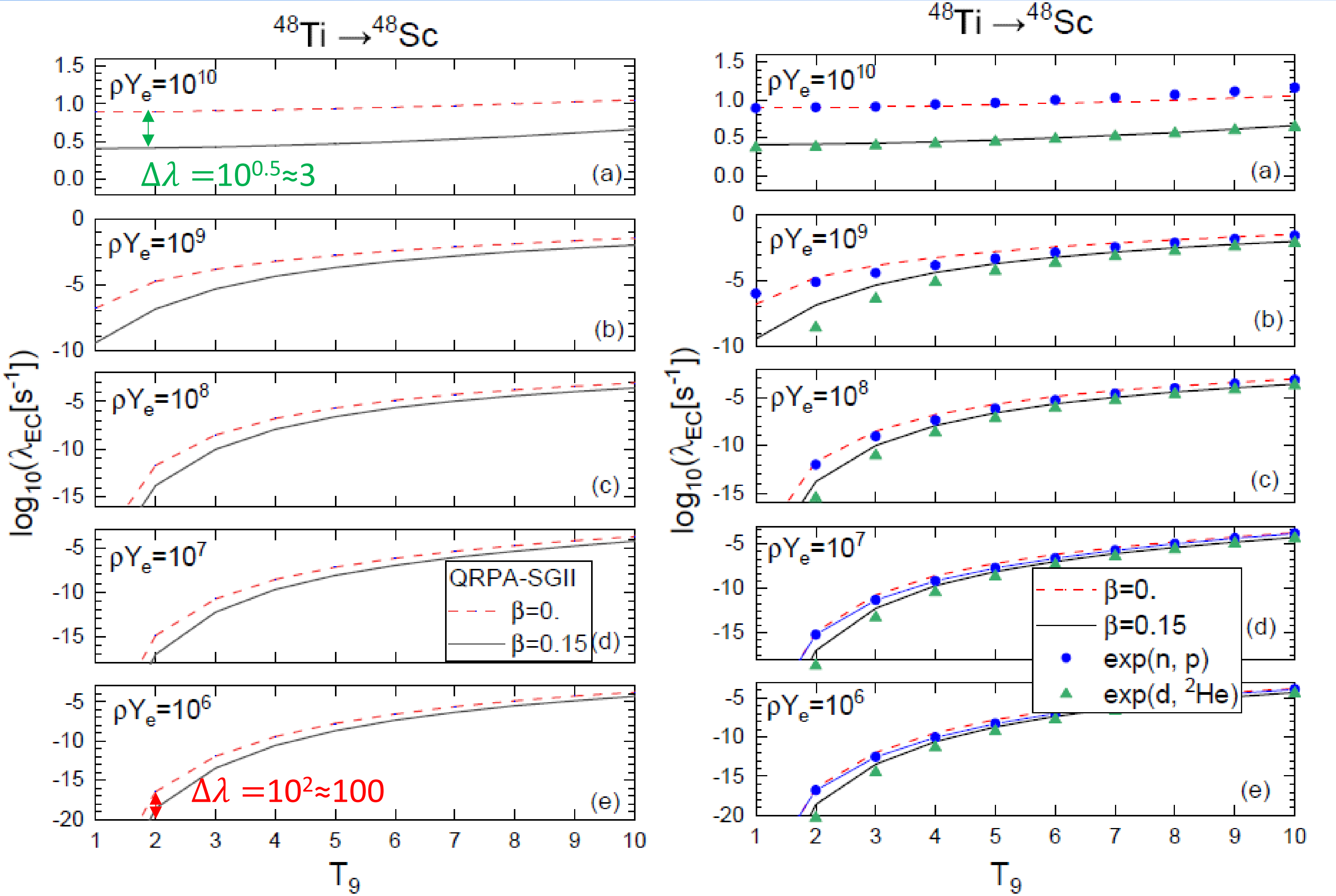

✓ At high densities, EC rates show weak deformation dependence due to the large available phase space. At low densities and temperatures, the rates become sensitive to low-lying GT^+ strength. Therefore, intrinsic nuclear shape plays **a more important role in the low-density regime.**

❖ B(GT) of ^{56}Ni

preliminary

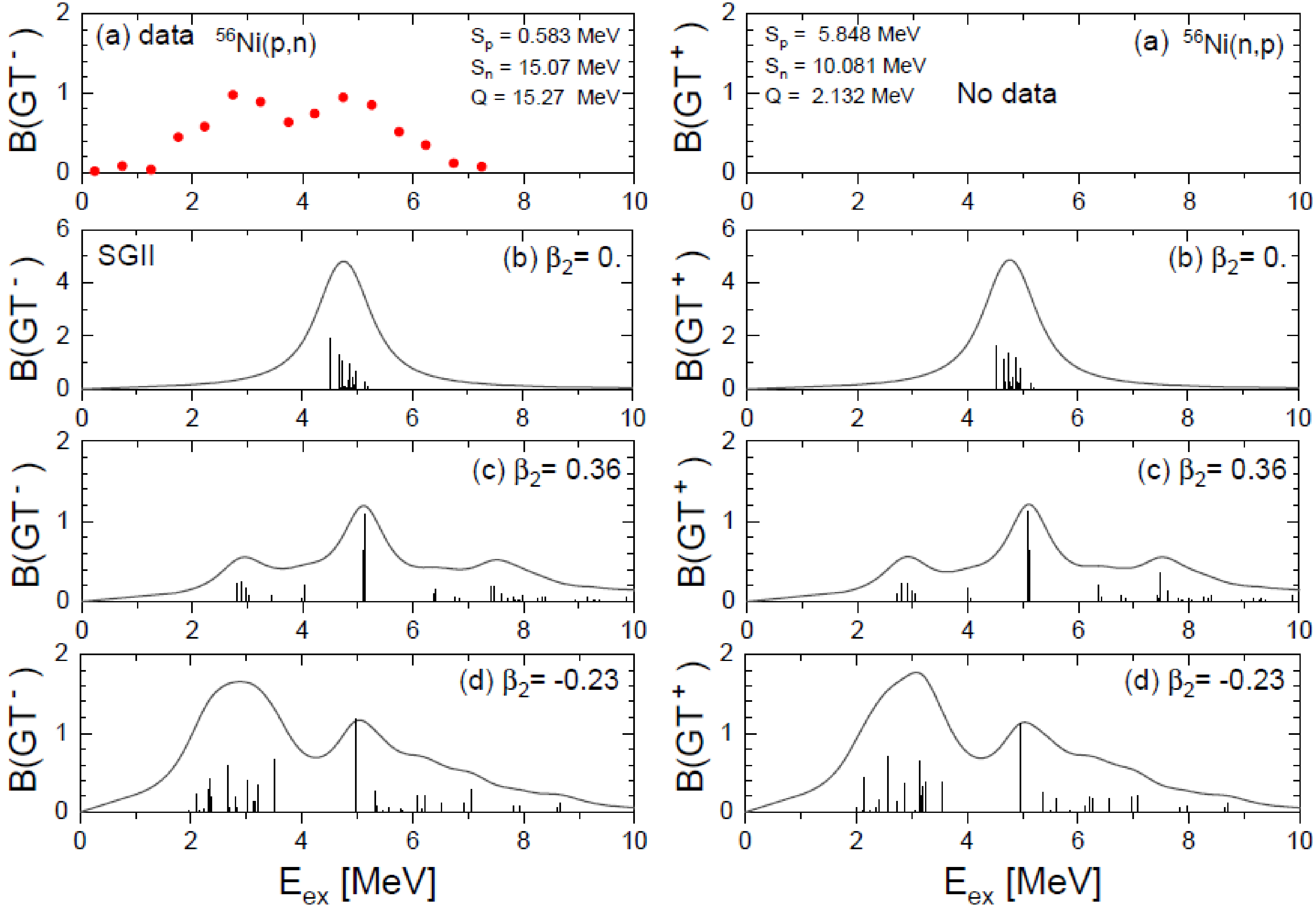

late case.

- ✓ The oblate configuration enhances the low-energy strength and yields a broader distribution, which appears to be qualitatively closer to the experimental trend than the pure spherical solution.
- ✓ The observed GT response in ^{56}Ni is not consistent with a single rigid spherical configuration.

❖ EC rate of ^{56}Ni

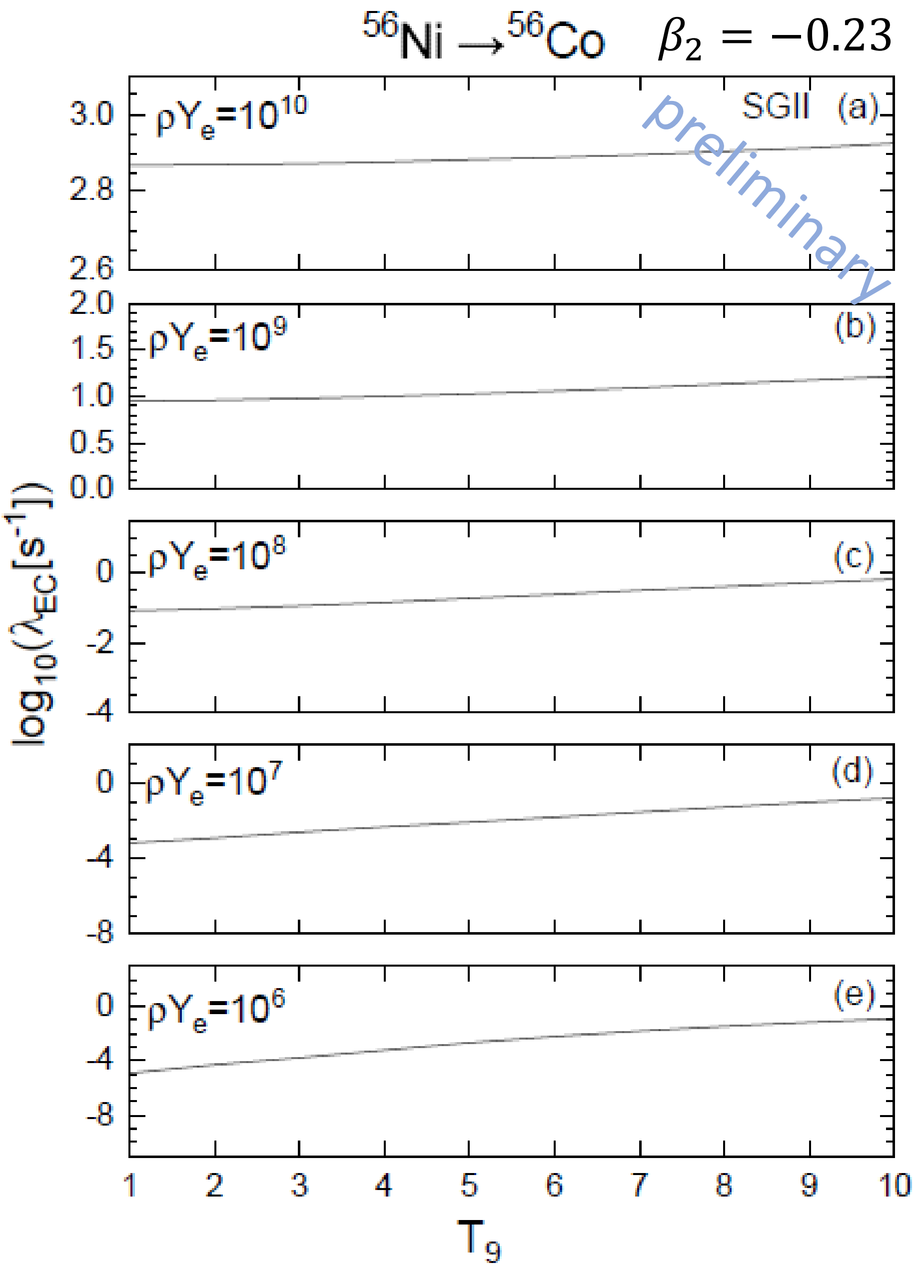

- ✓ EC rates in ^{56}Ni increase smoothly with temperature and density.
- ✓ The large electron phase space smooths out details of the GT strength.
  The positive Q_{EC} allows EC to occur easily, so the rates increase smoothly and show little shape dependence.
- ✓ The shape coexistence strongly affects GT spectroscopy, but only weakly affects the integrated EC rates.

❖ B(GT$^+$) & EC rate of ^{60}Zn

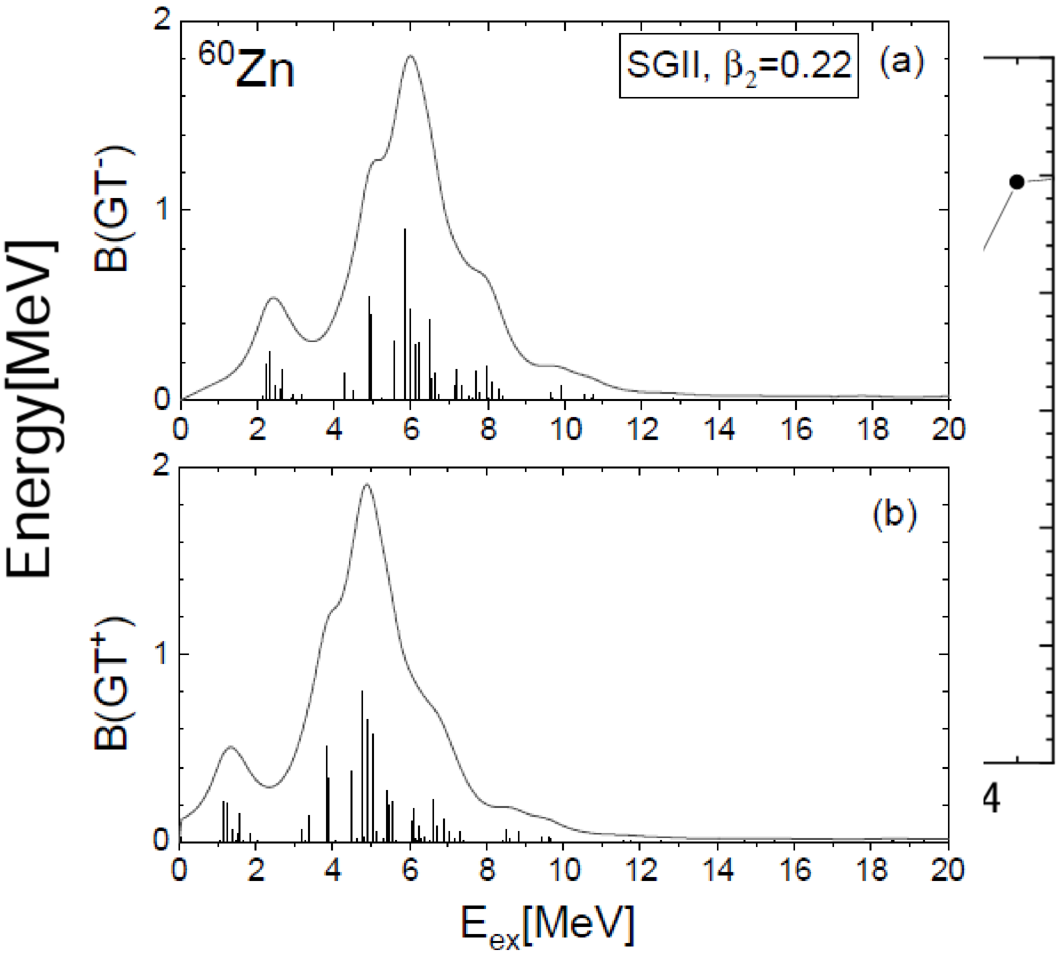

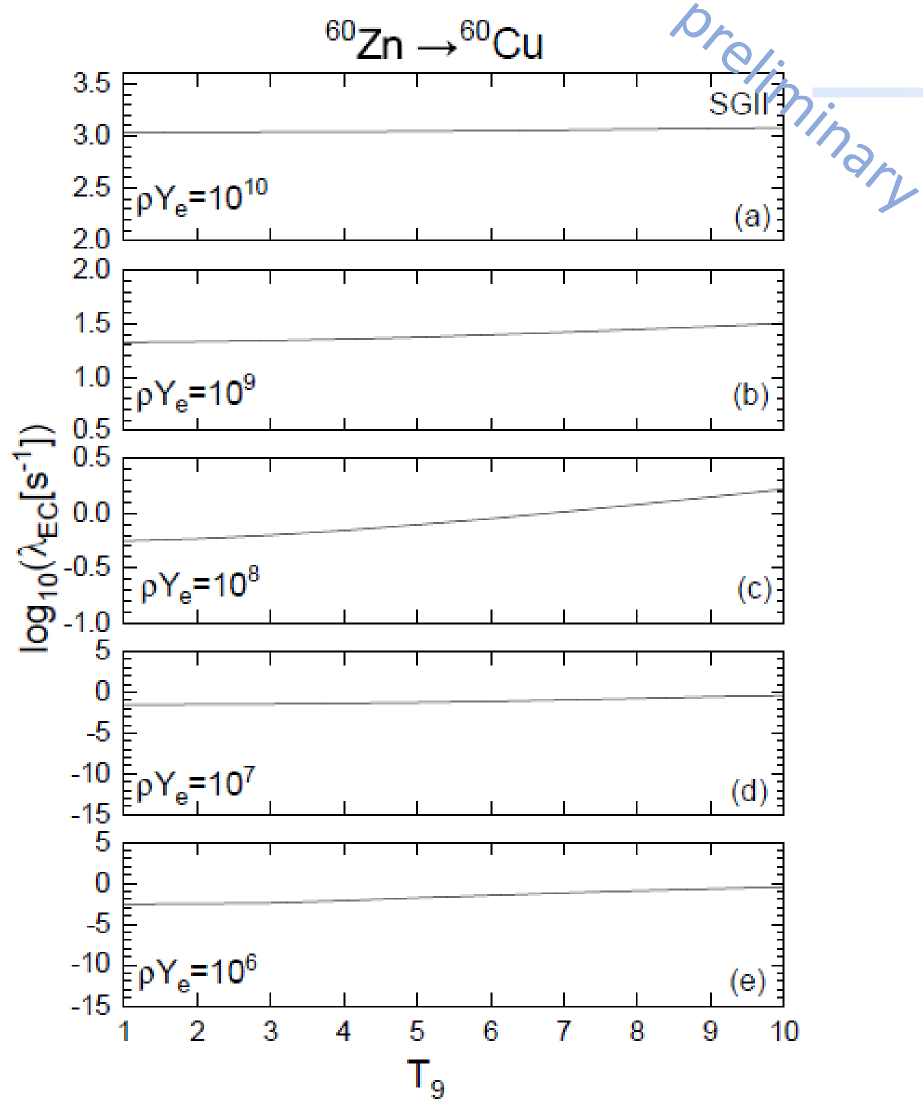

- ✓ A small energy, 1MeV, between $GT^+$and GT^-appears due to Coulomb and isospin-breaking effects. Because of its simple prolate structure, this shift is clearly visible in ^{60}Zn but masked in more fragmented nuclei such as ^{56}Ni and ^{64}Ge.
- ✓ EC rates in ^{60}Zn increase smoothly with temperature and density and remain largely insensitive to detailed GT fragmentation.

❖ B(GT$^+$) of ^{64}Ge

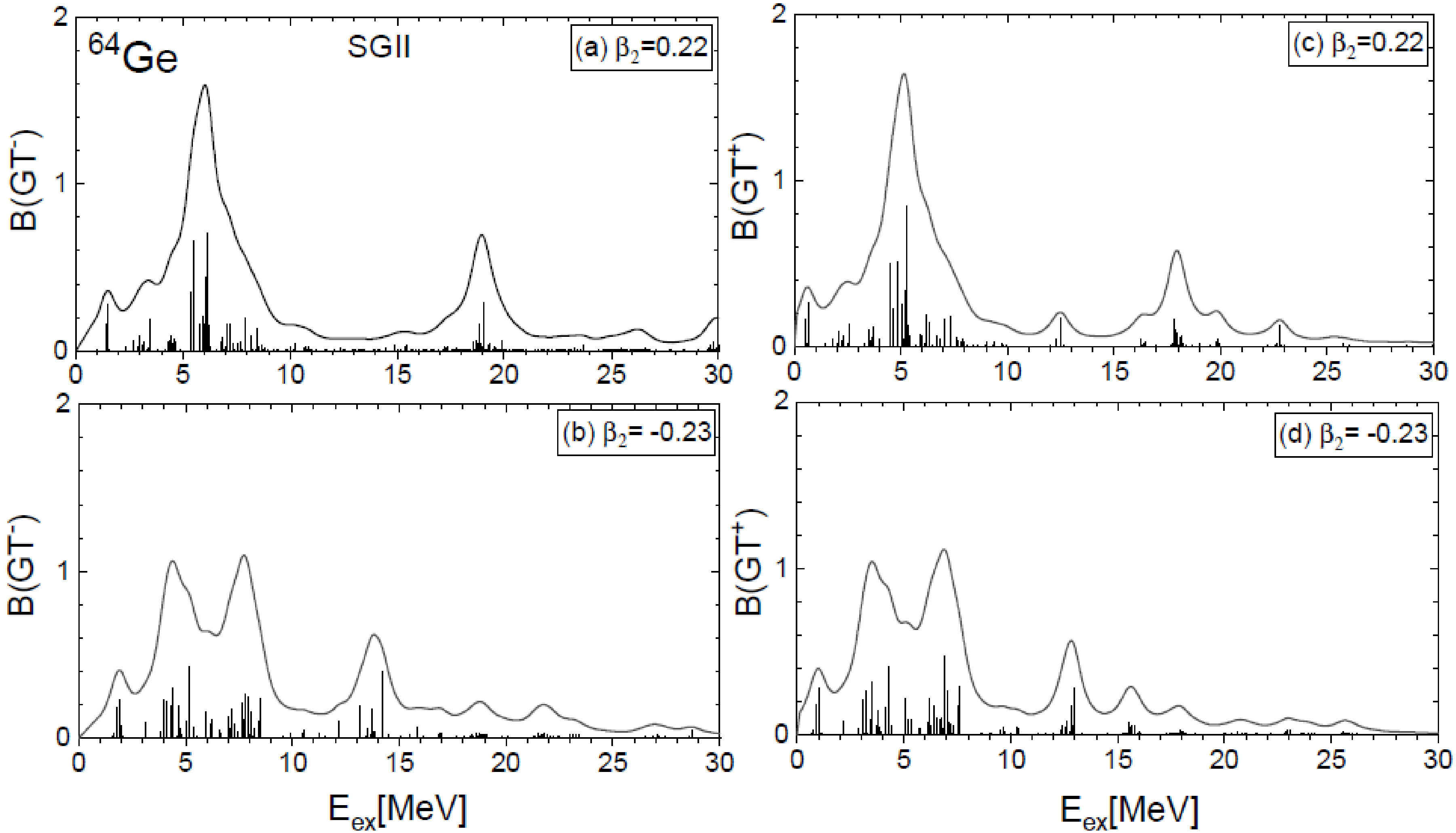

✓ In ^{64}Ge, nuclear shape strongly affects the GT strength by changing its distribution and fragmentation. The prolate shape shows a concentrated low-energy peak, whereas the oblate shape exhibits a more fragmented and spread-out pattern.

❖ EC rate of ^{64}Ge

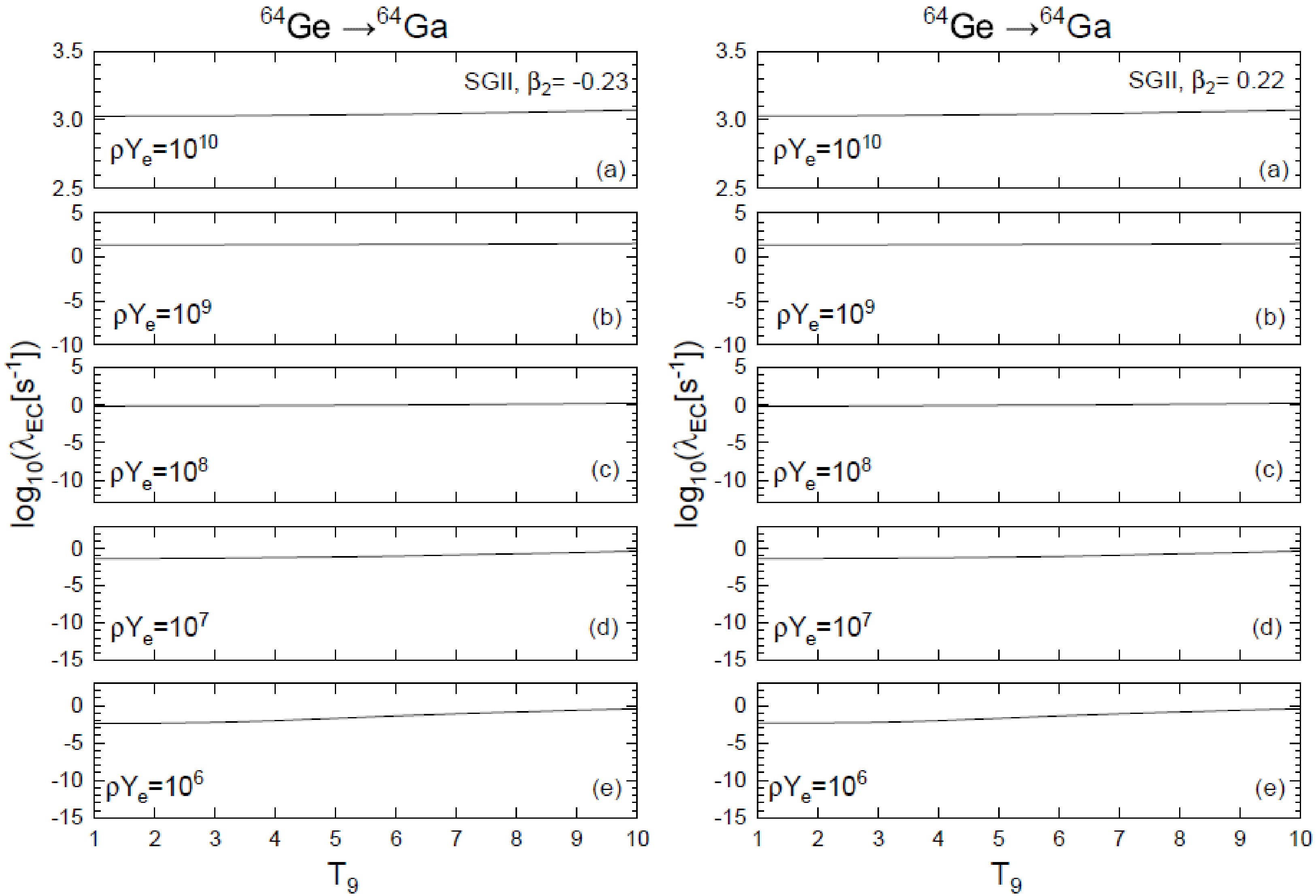

✓ The EC rates for different shapes remain nearly identical because the detailed GT structure is averaged out by the phase space. As a result, the rates are mainly sensitive to the overall low- and intermediate-energy strength.

❖ Electron chemical potential μ_e

$$\rho Y_e = \frac{1}{\pi^2 N_A}\left(\frac{m_e c}{\hbar}\right)^3 \int_0^\infty \left[S_e(\omega) - S_{e^+}(\omega)\right] p^2 dp,$$

where, ρ : baryon density, Y_e : electron fraction

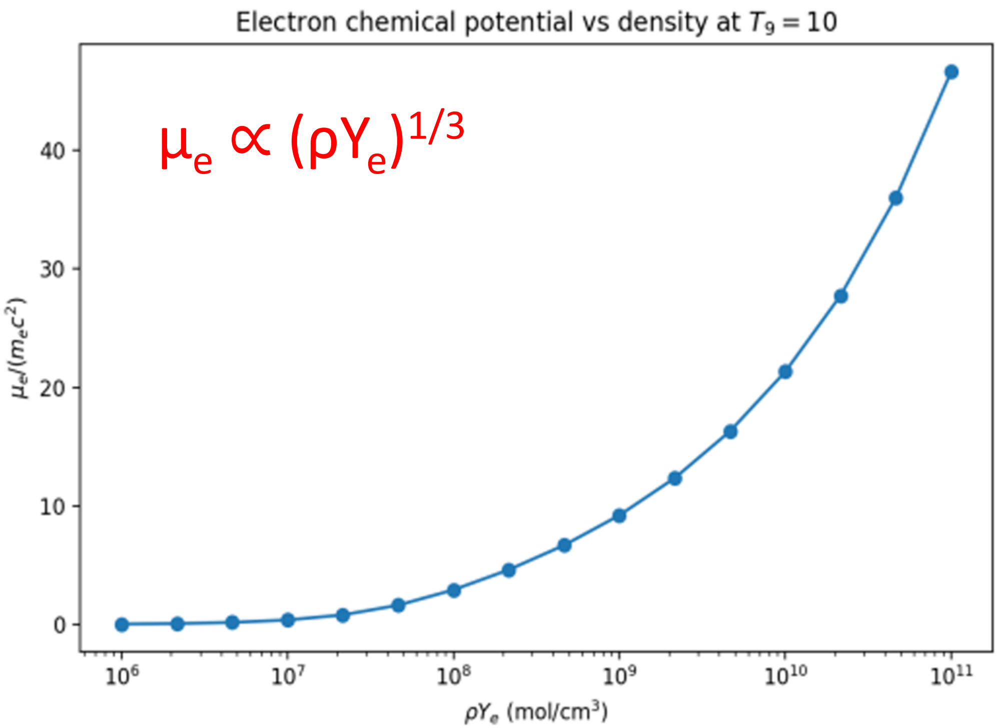

$$E_\nu = Q_{if} + E_e > 0$$

(1) $Q_{EC} < 0$ **(e.g.,** ^{48}**Ti)**

Electron capture requires high-energy electrons: $E_e \gtrsim |Q_{EC}|$.

When $\mu_e \ll |Q_{EC}|$: EC is strongly suppressed.

When $\mu_e \approx |Q_{EC}|$: EC rate increases rapidly.

(2) $Q_{EC} > 0$ **(e.g.,** ^{56}**Ni)**

The reaction is always energetically allowed.

When $\mu_e \sim Q_{EC}$:

- More electrons contribute to the phase space
- The EC rate increases more rapidly

✓ The electron chemical potential determines how many electrons can take part in EC. This sets the phase space and controls how the EC rate changes with density.

❖ Summary

1. We investigate the deformation dependence of GT strengths and stellar EC rates in ^{48}Ti, ^{56}Ni, ^{60}Ge, and ^{64}Zn.

2. Nuclear deformation changes the GT strength, including its distribution and fragmentation pattern.

3. EC rates are mostly insensitive to deformation because phase space averages out these details.

4. At low density and temperature, EC rates become sensitive to low-energy GT strength and nuclear shape.

5. The electron chemical potential controls the phase space and the density dependence of EC rates.

Thank you.

Back Up

❖ Why Gamow-Teller transition?

- **CE(charge-exchange)** reaction is very useful to study the **spin-isospin** **excitations** of nuclei.

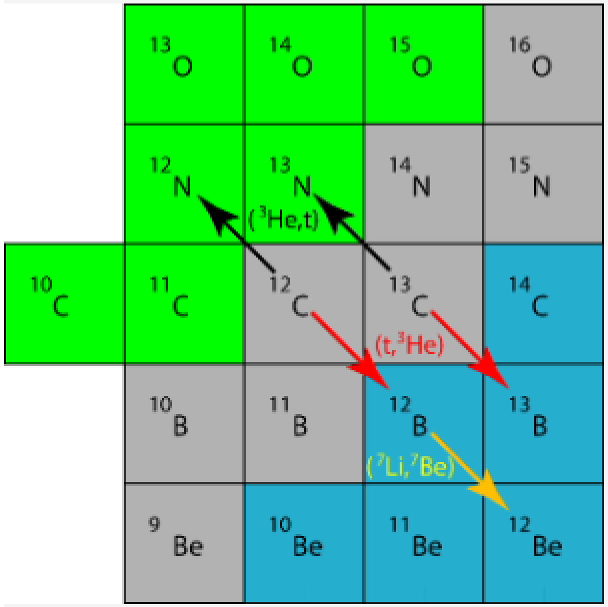

Gamow-Teller(GT) transition

The simplest spin-isospin excitation of a nucleus.

- Main transition in the $\nu - A$ reaction in nucleosynthesis.
- Model independent.
- For testing a new theoretical models of nuclei and nuclear force(weak interaction).
- B(GT) is related to the half-life of an allowed β-decay.
- NME(nuclear matrix elements) in $2\nu\beta\beta$ and $0\nu\beta\beta$-decay.
- There still remained some ambiguities in the NME.

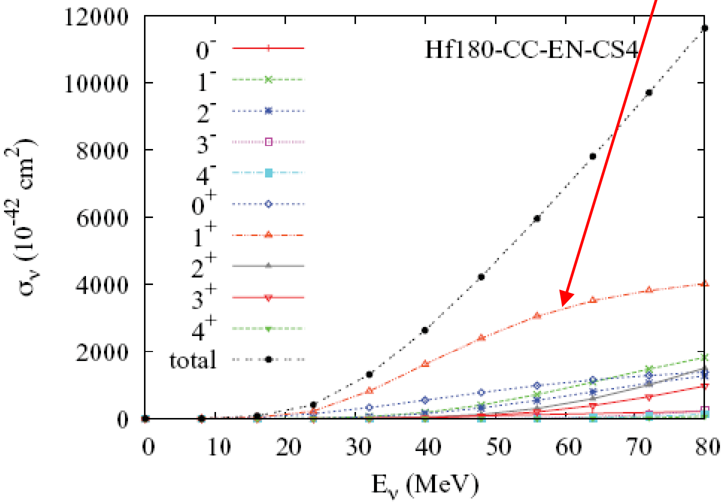

CHEOUN,HA,..PRC 82(2010)

Particle astro physics
Majorana ν, m_ν CP

$$T^{0\nu} = G^{0\nu}\,[M^{0\nu}\ m_\nu]^2$$

EXP

NNR,
Nucl. phys. g_A
short-range &
τ σ correlation

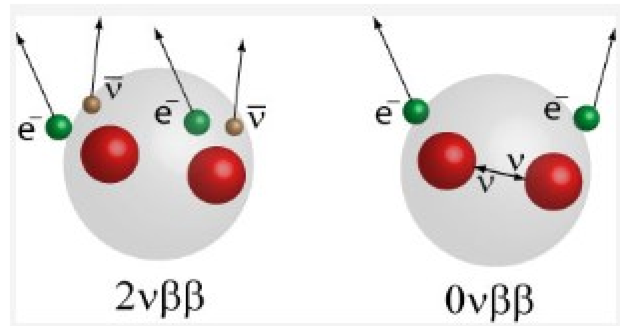

❖ SHFB: HFBTHO(v1.66p)

3 Skyrme Hartree-Fock-Bogoliubov Method

3.1 Skyrme Energy Density Functional

For Skyrme forces, the HFB energy (6) has the form of a local energy density functional,

$$E[\rho, \tilde{\rho}] = \int d^3\mathbf{r}\ \mathcal{H}(\mathbf{r}), \tag{9}$$

where

$$\mathcal{H}(\mathbf{r}) = H(\mathbf{r}) + \tilde{H}(\mathbf{r}) \tag{10}$$

is the sum of the mean-field and pairing energy densities. In the present implementation, we use the following explicit forms:

$$\begin{aligned} H(\mathbf{r}) \;=\; & \tfrac{\hbar^2}{2m}\tau + \tfrac{1}{2}t_0\left[\ \left(1+\tfrac{1}{2}x_0\right)\rho^2 - \left(\tfrac{1}{2}+\ x_0\right)\sum_q \rho_q^2\ \right] \\ + \; & \tfrac{1}{2}t_1\left[\ \left(1+\tfrac{1}{2}x_1\right)\rho\left(\tau - \tfrac{3}{4}\,\Delta\rho\right)\right] - \left(\tfrac{1}{2}+\ x_1\right)\sum_q \rho_q\left(\tau_q - \tfrac{3}{4}\Delta\rho_q\right)\Big] \\ + \; & \tfrac{1}{2}t_2\left[\ \left(1+\tfrac{1}{2}x_2\right)\rho\left(\tau + \tfrac{1}{4}\Delta\rho\right) - \left(\tfrac{1}{2}+\ x_2\right)\sum_q \rho_q\left(\tau_q + \tfrac{1}{4}\Delta\rho_q\right)\right] \\ + \; & \tfrac{1}{12}t_3\rho^\alpha\left[\left(1+\tfrac{1}{2}x_3\right)\rho^2 - \left(x_3+\tfrac{1}{2}\right)\sum_q \rho_q^2\right] \\ - \; & \tfrac{1}{8}\left(t_1x_1+t_2x_2\right)\sum_{ij}\mathbf{J}_{ij}^2 + \tfrac{1}{8}\left(t_1-t_2\right)\sum_{q,ij}\mathbf{J}_{q,ij}^2 \\ - \; & \tfrac{1}{2}W_0\sum_{ijk}\varepsilon_{ijk}\left[\rho\nabla_k\mathbf{J}_{ij} + \sum_q \rho_q\nabla_k\mathbf{J}_{q,ij}\right] \end{aligned} \tag{11}$$

and

Next goal is to include np-pairing.

$$\tilde{H}(\mathbf{r}) = \tfrac{1}{2}V_0\left[1 - V_1\left(\frac{\rho}{\rho_0}\right)^\gamma\ \right]\left[\sum_q \tilde{\rho}_q^2 + \sum_{qq'}\left(\tilde{\rho}_{qq'}^2 + \tilde{\rho}_{q'q}^2\right)\right] \tag{12}$$

Index q labels the neutron ($q=n$) or proton ($q=p$) densities, while densities without index q denote the sums of proton and neutron densities. $H(\mathbf{r})$ and $\tilde{H}(\mathbf{r})$ depend on the particle local density $\rho(\mathbf{r})$, pairing local density $\tilde{\rho}(\mathbf{r})$, kinetic energy density $\tau(\mathbf{r})$, and spin-current density $\mathbf{J}_{ij}(\mathbf{r})$: